NJC

Accepted Manuscript

This is an *Accepted Manuscript*, which has been through the Royal Society of Chemistry peer review process and has been accepted for publication.

Accepted Manuscripts are published online shortly after acceptance, before technical editing, formatting and proof reading. Using this free service, authors can make their results available to the community, in citable form, before we publish the edited article. We will replace this *Accepted Manuscript* with the edited and formatted *Advance Article* as soon as it is available.

You can find more information about *Accepted Manuscripts* in the Information for Authors.

Please note that technical editing may introduce minor changes to the text and/or graphics, which may alter content. The journal's standard Terms & Conditions and the Ethical guidelines still apply. In no event shall the Royal Society of Chemistry be held responsible for any errors or omissions in this *Accepted Manuscript* or any consequences arising from the use of any information it contains.

ROYAL SOCIETY OF CHEMISTRY

www.rsc.org/njc

NJC

RSCPublishing

ARTICLE

Preparation and characterization of nano-1, 1 Diamino-2, 2-dinitroethene (FOX-7) explosive

Cite this: DOI: 10.1039/x0xx00000x

Bing Gao, †[abc] Peng Wu,[a] Bing Huang,[a] Jun Wang, †[a] Zhiqiang Qiao,[a] Guangcheng Yang*[ab] and Fude Nie*[a]

Received 00th January 2012,
Accepted 00th January 2012

DOI: 10.1039/x0xx00000x

www.rsc.org/

Nano-1,1-Diamino-2,2-dinitroethene (FOX-7) explosive particles were successfully prepared via ultrasonic spray-assisted electrostatic adsorption (USEA) method and sub-micro FOX-7 were also obtained by recrystallization (absolute ethyl alcohol as solvent) for comparison. The samples were characterized by Field emission scanning electron microscopy (FE-SEM), X-ray diffraction (XRD), Fourier transform infrared spectroscopy (FT-IR), Atomic force microscope (AFM) and particle size and size distribution. The results show that there are two groups of size distribution in the range from 30 to 200 nm for the nano-sized FOX-7 prepared by USEA method, and the average particle size of FOX-7 is approximately 78 nm. While, sub-micro FOX-7 particles obtained via recrystallization are in a single size distribution of 200-450 nm. The particles were cubic and spheroidic, respectively. What's more, their thermal properties were also investigated by Differential scanning calorimetry (DSC) and Thermogravimetry (TG). For nano-sized FOX-7, the first exothermal peak is 267.4℃ increased by 45℃ and is fast energy release efficiency and more release energy compare to original and sub-micro particles crystals (222.7℃), there is a potential alternative application for micro electro mechanical systems (MEMS), micro thrusters and so on.

1. Introduction

1,1-Diamino-2,2-dinitroethene ($C_2H_4N_4O_4$) commonly called FOX-7 is a thermally stable insensitive munition (IM) high-energy materials developed by the Swedish Defence Research Agency in 1998.[1-3] It has been reported to be an energetic high explosive nitroenamine which is suggested as a potential replacement for the currently used secondary explosive cyclo-1,3,5-trimethylene-2,4,6-trinitramine ($C_3H_6N_6O_6$, RDX) and 1,3,5,7-tetranitro-1,3,5,7-tetrazoctane ($C_4H_8N_8O_8$, HMX), due to its higher threshold toward impact and friction sensitivity.[4-8] Many researchers have focused their eyes on the theoretical calculation, synthesis, thermal properties by now,[2,9-11] whereas few studies are on the nanostructures of FOX-7. As we all known that nano materials have unique large surface area and extraordinary properties, the structures, compositions, sizes and shapes, are of great difference at the atomic and molecular scale.[12-14] The use of nano technology has provided a great approach in military and industrial applications, especially in the area of nano energetic materials, such as RDX,[15-17] HMX,[18-20] 2,4,6-triamino-1,3,5-trinitrobenzene (TATB),[21-23] 2,4,6,8,10,12-hexanitro-2,4,6,8,10,12-hexaazaisowurtzitan (CL-20),[24,25] 3-nitro-1,2,4-triazol-3-one (NTO).[26] And nano-sized

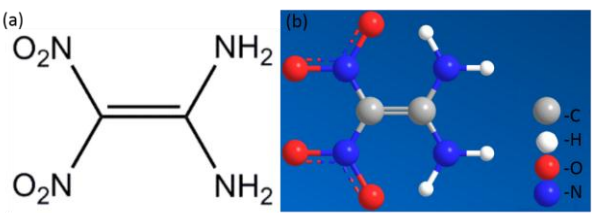

Fig. 1 Planar structure of FOX-7 (a) and crystal structure of FOX-7 (b). C, H, O, and N atoms are indicated in grey, white, red, and blue, respectively.

FOX-7, as a very promising alternative energetic material, may be widely used in micro electro mechanical systems (MEMS),[27-29] micro thrusters,[30-31] and so on, in particular.

In the recent years, some works have been done for the properties of FOX-7, Huang et al.[32] of our groups have fabricated FOX-7 quasi-three-dimensional grids of one-dimensional nano structures via spray freeze-drying method together with the size-dependence's thermal properties in 2010, Thao T. Vo et al.[33] made Copper and Nickel Diamine Complexes and Copper FOX-7, the samples are less sensitive to

[a] Institute of Chemical Materials, China Academy of Engineering Physics (CAEP), Mianyang 621900, PR China

[b] Si Chuan Research Center of New Materials, Mianyang 621000, PR China

[c] School of Material Science and Engineering, Southwest University of Science and Technology, Mianyang 621010, PR China

†These authors contributed equally to this work.

impact as expected. Alok Kumar Mandal et al.[34] also provided another way for the preparation of spherical particles of FOX-7 using a Micellar Nanoreactor. What's more, Cai et al.[35] has made a novel FOX-7 nanocrystals by embedding FOX-7 in mesoporous carbon FDU-15, the result shows that the extreme insensitivity is closely related to the high thermal and mechanical stability of FDU-15.

There are many techniques which have been used to reduce the particle size of materials. However, most methods are only in small doses. Milling methods,[36,37] as the classical nano crystal technology, are known as a top-down approach to nano world from the first half of the 20th century, which can be equipped widely into industry. The materials to be crushed are added in the form of a powder of about 50-100 μm diameter grain size and the milling time can last from about 30 minutes to hours or to several days depends on different drugs and other factors, such as the surfactant content, hardness of the materials, viscosity, temperature, energy input, size of the milling media.[38-41] However, besides the high output of heat and threshold toward impact and friction sensitivity for energetic materials, security is another key consideration and discussion which need to be noticed. Unfortunately, the heat release is not controllable in milling methods. Moreover, inevitable impact and friction go with the reduction of products is also occurred, so a further improvement of great scale and safety operation in preparing nano energetic materials is needed.

Ultrasonic spray-assisted electrostatic adsorption (USEA) method has been demonstrated as a simple and continuous method for the preparation of nano-/sub-micro-sized particles, based on droplet recrystallization under the influence of gradient evaporation.[17,42] Compared with other chemistry methods, USEA provides a facile approach to generate relatively uniform nano/micro particles.[43,44] Other methods can also assemble nanoparticles into microspheres.[45,46] But uniquely, the USEA method has the advantage of producing nano/micro particles with a narrow size distribution. Additionally, the possible control and tuning of solution concentration, ultrasonic transducer frequencies and working temperatures by USEA method can prepare different size particles from nano to micro meters. Furthermore, it is also a very effective alternative for industrial by this electrostatic assist, making this approach particularly useful to produce other small-molecule organic materials.

The objective of this study was to develop a new and continuous method of the atomization process for the preparation of FOX-7 explosive nano-/sub-micro-sized particles for the first time via ultrasonic spray-assisted electrostatic adsorption (USEA) method as the part of evaporative crystallization. An ultrasonic nebulizer is used to generate the aerosol in which a piezoelectric transducer is located at the centre bottom of the container. When the piezoelectric transducer is switched on, ultrafine droplets are generated on the upper liquid surface, because of the qualification caused by ultrasonic waves generated in the liquid. The mechanism of ultrasonic atomization has been studied by Robert Lang.[47] The droplet size can be estimated reasonably and accurately using Lang's equation:

$$d_p = 0.34(8\pi\sigma/\rho f^2)^{1/3} \quad (1)$$

where d_p: the droplet size, σ: surface tension (dyne/cm), ρ: density (g/ml), f: excitation frequency (Hz). A constant fraction of 0.34 of certain frequencies from 10 to 800 kHz is given.[48] The capillary wavelength is calculable by Kelvin's equation using the exciting frequency and the properties of the fluid being atomized. There is a good correspondence between capillary wavelength and droplet size, the capillary wavelength increases slowly with liquid phase viscosity. Although Lang's study is only limited to the low frequency, many studies[49-51] have shown that the particle size might be directly related to the wavelength of these capillary waves. Herein, we report a method for the preparation of nano FOX-7 explosive which may be helpful for the potential use in military and industrial application areas.

2. Experimental section

2.1 Materials

1,1-Diamino-2,2-dinitroethene (FOX-7, $C_2H_4N_4O_4$) explosive (purity =99. 6%, particle size 4-20 μm) were obtained from our own laboratory. Acetone (CH_3COCH_3, AR grade) and absolute ethyl alcohol (CH_3CH_2OH, AR grade) were obtained from Chengdu United Chemical industry (Chengdu, China). High purity nitrogen (N_2, 99.999%) was bought from Changjun GAS CO.,LTD (Mianyang, China), The ultrasonic nebulizer (402-B) with a series of Ultrasonic frequency was supplied by YUYUE medical CO.,LTD. (Jiangsu, China), and the Work Voltage is 220 V, the ultrasonic transducer frequency is 1.7 MHz ± 0.17 MHz.

2.2 Sample preparation

2.2.1 Preparation of sub-micro-sized FOX-7

Sub-micro FOX-7 particles were prepared by recrystallization, about 0.10 g of raw FOX-7 is dissolved into 50.0 ml absolute ethyl alcohol (solvent) and under stirring (300 rpm) at 60℃ for one hour, and following by a state of static settlement for another hour. After filtration, lavation, and air-drying at room temperature, the recrystallized sub-micro FOX-7 samples with regular morphology were obtained.

2.2.2 Preparation of nano-sized FOX-7

0.10 g of raw FOX-7 is dissolved into 50.0 ml acetone (solvent), in a concentration below the saturation point at 25℃. The ultrasonic spray-assisted electrostatic experimental installation which was designed by our own laboratory is shown in Fig. 2. There are three main components: (I) ultrasonic spray. It is used to generate an aerosol on the upper liquid surface of the solution and (II) an oven which is heated differently with different zones. The half of the oven close to the entry is in hot surroundings with a maximum temperature of 90-120℃ and attenuate to 60-80℃ towards the other half of the oven. The oven is heated by the heater band which tightly bound around

the oven. (III) Electrostatic adsorption precipitator composed of two electrodes between which an electrostatic field would be

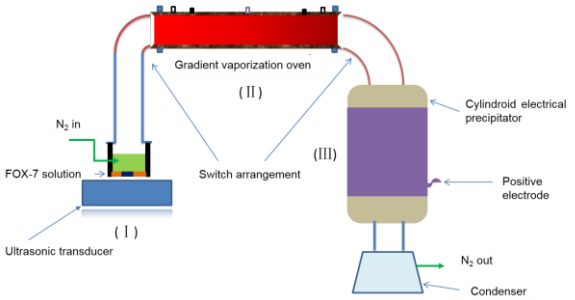

Fig. 2 A brief representation of the apparatus.for nano FOX-7 by UESA method.

existed once the switch turned on. According to security consideration and balancing the efficiency of the installation, the minimum distance of the two electrodes is not less than 9.0 cm. When ultrasonic spray is turned on, aerosols are produced on the upper of the solution, the aerosols quantity is affected by the frequency as well as the liquid level, then the aerosols are transported by the inert gas (nitrogen) towards the container and turn into droplets.

When the droplet enters the oven which is differently heated in a different zones, crystallization process of nano-FOX-7 is quickly completed with the evaporation of the solvent. Varied sizes of droplets get a complete crystal growth, as a result of unequal heating. The nanoparticles of FOX-7 flow out of the oven with the help of the gas and continue to be dried at the temperature 60 ± 1℃ (higher than the boiling point of acetone). Nano FOX-7 was adsorbed via directional movement from the anode to cathode under the force of electrostatic attraction (electrical tension: 0-5 kV). The particles are accumulated mainly close to the bottom of the precipitator. There are few nano particles to be stored in the electrostatic adsorption precipitator, because the particles almost adhere to the inwall of the oven at the first hour of the experiment. The production rate is constant for a given work parameters.

2.3 Characterization

2.3.1 Field emission scanning electron microscopy (FE-SEM). The morphology and surface appearance of the nano FOX-7 particles were characterized by field emission scanning electron microscopy (FE-SEM, Ultra-55, Carl Zeiss, Germany) at an acceleration voltage of 10 kV after gold sputtering coating under the vacuum degree of 10^{-6} Pa for 50 seconds.

2.3.2 Particle size and size distribution. The average size and particle size distribution of FOX-7 were calculated by means of counting more than 300 particles from the obtained SEM images via the statistics of the smileview software.

2.3.3 X-ray diffraction. The phase content of FOX-7 was determined by X-ray diffraction (XRD, X'Pert Pro, PANalytical, The Netherlands) analysis using Cu-Kα (λ= 1.540598 Å) radiation at 50 kV and 30 mA and a graphite diffracted-beam monochromatic. The samples were packed into an amorphous silicon holder and the diffraction angle (2θ) scanned from 5° to 80° , The scanning rate was 10 °·min^{-1}.

2.3.4 Fourier transform infrared spectroscopy (FT-IR) FT-IR spectrum was recorded on a Bruker-Tensor 27 spectrometer (FT-IR, bruker, Germany). About 150 mg of KBr was ground in a mortar and pestle, and 1 wt % of the solid sample was ground with KBr in the region 4000-400 cm^{-1}.

2.3.5 Atomic force microscope. The imaging of nano-RDX was carried out in ambient conditions on a SPA300HV Atomic force microscope (AFM, SPA300HV, Japan). Equipped with a piezoelectric ceramics scanning head. The tapping mode was used with a length of 10×10 μm and a spring constant of 40 N·m^{-1}.

2.3.6 Differential scanning calorimetry and thermogravimetry. Samples of raw FOX-7 and prepared FOX-7 were analysed with a Differential Scanning Calorimetry and thermogravimetry TG (DSC/TG, PerkinElmer Diamond, America). The conditions were as follows: sample mass: 3.00 mg; heating rate: 10 K•min^{-1}; nitrogen atmosphere (flow rate: 30 mL·min^{-1}).

3. Results and discussion

3.1 Structural characterization

The molecular structure of nano-sized FOX-7 and raw-FOX-7 was confirmed by powder XRD patterns. As shown in Fig. 3 (grey), the peaks observed at 2θ=26.8°, 28.1°, and 20.1° are assigned to the (020), (021), (111) reflection lines of the raw FOX-7 and exhibits a

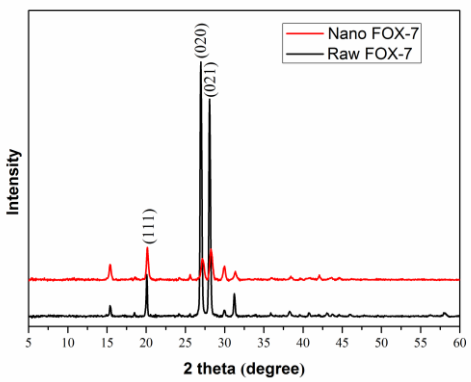

Fig. 3 XRD diffraction patterns of the raw FOX-7 (gray) and prepared FOX-7 (red) by USEA method.

high crystallinity. These values are in good agreement with the diffraction peaks. For the peaks of nano FOX-7 presented in Fig. 3 (red), the location of (020), (021), (111) diffraction peak which is presenting the three strongest in its intensity were almost unchanged, indicating that the prepared productions are still FOX-7 explosives. [35]

To obtain more quantitative information of the prepared FOX-7 nanoparticles, the average particle size can be calculated by inserting the width at half height of the signals in the Debye-Scherrer equation:[52]

$$L=0.89\lambda/(\beta\cos\theta) \qquad (2)$$

where L is the coherence length (nm), β is the full width at half maximum (FWHM) of the peak, λ is the wavelength of the X-ray radiation (1.540598 Å), and θ is the angle of diffraction peak. Though the peaks are weak, the obtained average ***L*** value is 36 nm.

The FT-IR spectroscopy of FOX-7 was carried out to further characterize the FOX-7 structure. FT-IR spectra of raw FOX-7 (Fig. 4a), sub-micro FOX-7 (Fig. 4b) and nano FOX-7 (Fig. 4c) showed the characteristic band of the $-NH_2$ and $-NO_2$ functional group wavenumber ranges in the 3220-3416 cm^{-1} and 1332-1620 cm^{-1}, respectively, together with numerous peaks in the fingerprint region.

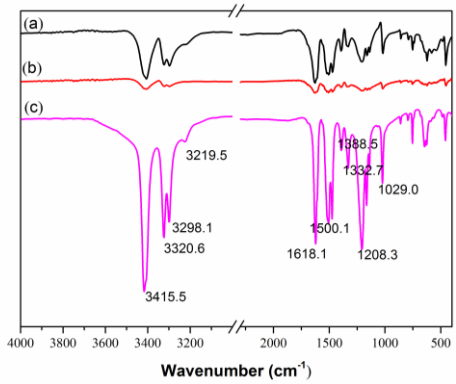

Fig. 4 FT-IR spectra of Raw-FOX-7 (a), sub-micro FOX-7 obtained by recrystallization (b) and nano FOX-7 prepared by USEA method.

3.2 Morphology and particle size characterization

The morphology and particle size of FOX-7 were observed and revealed by FE-SEM and AFM characterizations. In order to detect differences in their surfaces. The FE-SEM images of raw FOX-7 (Fig. 5C), sub-micro FOX-7 (Fig. 5A), and nano FOX-7 (Fig. 5B) were studied together with their particle sizes and average particle size which measured from the FE-SEM image, as shown in Fig. 5. The FE-SEM images indicate that the samples of FOX-7 prepared via recrystallization (absolute ethyl alcohol as solvent) and USEA methods still retain the structural integrity. However, the morphology of particles prepared by recrystallization and USEA method are greatly different appearance from the original particles' long-prismatic shape, were cubic and spheroidic, respectively.

In particular, the samples obtained by recrystallization from absolute ethyl alcohol are a certain degree of agglomeration but homogeneous which in accordance with the relative broad distribution of particle size from 200 nm to 450 nm and the average particle size is 340 nm (Fig. 5 (a)). While, it is obviously observed that the particle size of FOX-7 prepared via USEA method is reduced (Fig. 5 (c)) and the suitable particle size & size distribution of the prepared nano particles is also given shown in Fig. 5 (b) and the average particle size is 78 nm. Moreover, its particle size distribution is relatively narrow with 30-200 nm of smaller size compared with raw FOX-7. Specially, no obvious particle aggregation was observed from the SEM images of the samples prepared via USEA method. The possible reasons can be explained that the chaotic and complex aerosol size distribution generated by the piezoelectric transducer at the aerosol production process makes the aerosol size's difference and its distribution.[48] Thus, small aerosol size droplets crystallize small particles and at the same time, big aerosol size droplets crystallize big particles in the crystallization step. What's more, the repulsive force existing in

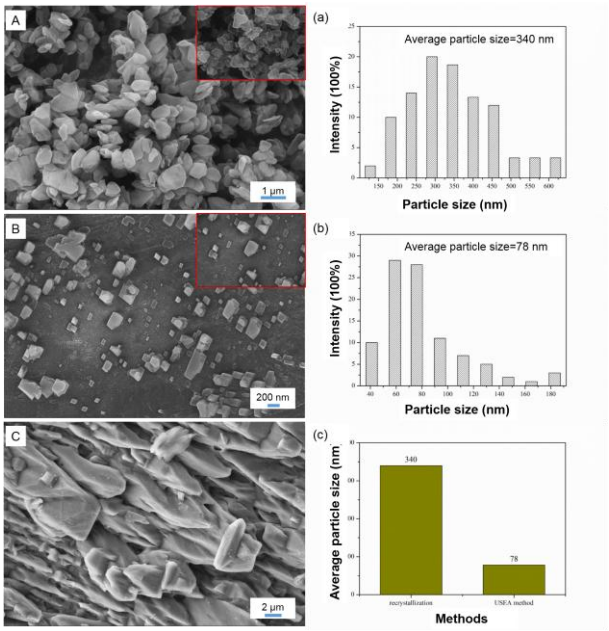

Fig. 5 SEM images and particle sizes of sub-micro FOX-7 (A, (a)) prepared by recrystallization absolute ethyl alcohol as solvent, nano FOX-7 (B, (b)) prepared by USEA method at the voltage of 5kV, ultrasonic transducer frequency of 1.7 MHz, and the raw FOX-7 (C),

the electrostatic field of each particle reduces the agglomeration of crystals with each other. And through the effect of ultrasound can help diminish the size to a certain extent, the main contribution of being nano size involves the rupture of the capillary surface waves and the subsequent ejection as droplets of the wave peaks from the surface in the aerosol process.

To further demonstrate the morphology and particle size of the samples, we also examined nano-FOX-7 by atomic force micrographs (AFM) obtained by USEA method at the voltage of 5kV, ultrasonic transducer frequency of 1.7 MHz, as shown in Fig. 6 and Fig. 7.

The micrograph of Fig. 6 gives a global AFM registration of a relative large scanning area (10×10 μm), Fig. 6A shows that there are two kinds of particles sizes: elementary particles of about 30-90 nm, and agglomerates together with each other of about 100-200 nm. It can be also read clearly from the FE-SEM of Fig. 5B together with the magnification image attaching in the top right corner. A 3D view of the data in Fig. 6B shows that the height is about 20 nm. Fig. 7 gives the length analysis of the nano FOX-7 prepared by USEA method at the voltage of 5kV, ultrasonic transducer frequency of 1.7 MHz after dispersing the nanoparticles in a non-solvent diethyl ether.

The AFM microscopy of no vacuum and no heating needed, is considered the most suitable method for the

characterization. The sample is not destroyed during the observation.

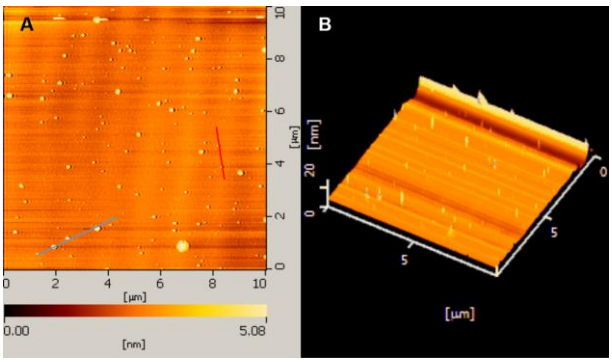

Fig. 6 AFM images and particle sizes of nano FOX-7 large registration scanning area imaging (A) prepared by USEA method at the voltage of 5kV, ultrasonic transducer frequency of 1.7 MHz after dispersing the nanoparticles in a non-solvent diethyl ether, and a 3D view of the data (B).

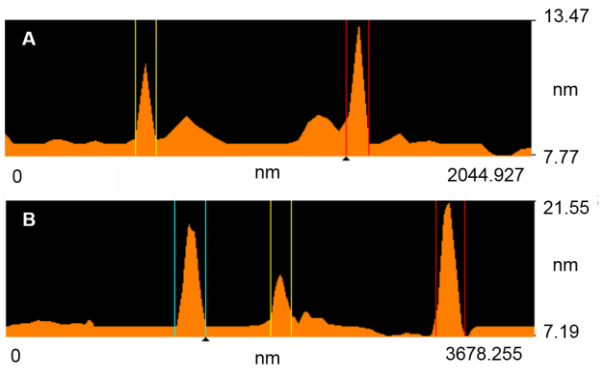

Fig. 7 AFM images of height measurements of nano FOX-7 elementary particles of about 30-90 nm (79 nm, 87 nm, surface analyze from left to right) (A), and agglomerates of about 100-200 nm (215 nm, 143 nm and 201 nm surface analyze from left to right) (B), drawing on the different surface of Fig. 6 (A-red, B-blue).

3.3 Thermal analysis and thermal stability properties

The thermal properties of the raw FOX-7 and prepared FOX-7 were investigated using differential scanning calorimetry (DSC) and thermogravimetry (TG) measurements. Fig. 8 shows the results of DSC curve of the raw FOX-7 (Fig. 8 (a)), sub-micro FOX-7 (Fig. 8 (b)), and nano FOX-7 (Fig. 8 (c)). From the DSC curve, we can see that the thermal behaviour of FOX-7 can be divided into three stages: (1) the pyrogenic decomposition for the raw and sub-micro FOX-7 in the range of 200-210℃, (2) the first exothermic decomposition stage occurs at 210-268℃ and (3) the second exothermic decomposition stage occurs at 280-292℃ for both raw and prepared FOX-7. Fig. 8 (a) and Fig. 8 (b) have the first similar signal above 200 ℃ (201.2 °C), it corresponds to the presence of amorphous FOX-7 particles, according to the Bellamy review,[1] while, there is no signal for nano FOX-7 which may indicate that the good degree of crystallinity for nano FOX-7.

In fact, the increasing of phase transition temperature is hard to be detected, most studies showed that the phase transition temperature is not found for nano FOX-7 particles.[10,32]

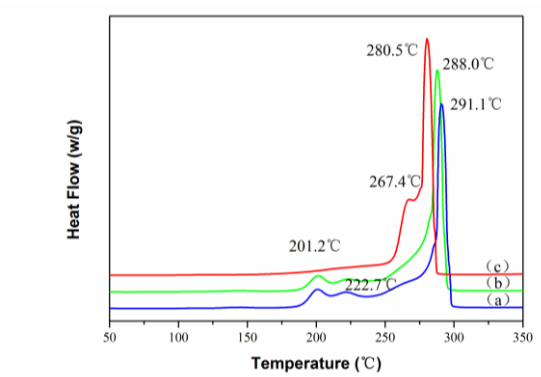

Fig. 8 DSC curve of the raw FOX-7 (a), sub-micro FOX-7 (b) prepared by recrystallization absolute ethyl alcohol as solvent, and nano FOX-7 (c) prepared by USEA method at the voltage of 5kV, ultrasonic transducer frequency of 1.7 MHz.

Exothermal reactions have been one of the most important explosive properties of current interest from the reports until now.[9,33,35,53] The other two stages are the exothermic decomposition processes: the first exothermal peak can be elucidated by the emergence of nitro-to-nitrite rearrangement in the molecule which leads to the destruction of conjugated system and hydrogen bonds and thus the fracture of nitro-result in the formation of nitrogen monoxide (NO),[54] and the second exothermal peak can be described as the fracture of carbon skeleton in FOX-7 molecule. The raw FOX-7 exhibited an obvious exothermic peak at 222.7℃ (first exothermal peak), with the same peak of sub-micro FOX-7, while, that peak shifts right to 267.4 ℃, increased by 45 ℃ for nano FOX-7. It can be

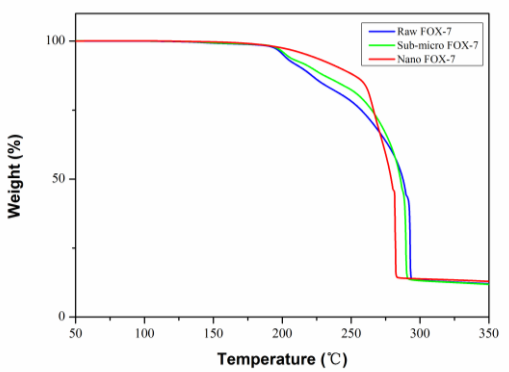

Fig. 9 TG curve of the raw FOX-7 (a), sub-micro FOX-7 (b) prepared by recrystallization absolute ethyl alcohol as solvent, and nano FOX-7 (c) prepared by USEA method at the voltage of 5kV, ultrasonic transducer frequency of 1.7 MHz.

clearly observed that this first exothermal peak shifts toward higher temperature with the decrease of FOX-7 particle sizes. This phenomenon can be explained by topochemical reactions theory,[55] generally, the smaller (nano) sized FOX-7 particle requires a higher decomposition temperature because of its less

lattice defects and smaller internal stress. As for the second strong exothermic peak, the T_{max} of raw and sub-micro FOX-7 are 291.1 ℃and 288.0℃, respectively. Both of them are higher than that of the nano FOX-7 (280.5℃), namely that there is a shift of 11℃and 7.5℃ to lower temperature. The result shows that the second peak of FOX-7 typically decreased with a decrease in size which is similar to the former works of others.[32,56] This probably caused by the increase of the ratio of surface atoms to interior atoms than raw and sub-micro FOX-7 which leads to a higher surface energy and results in the decrease of decomposition peak. What's more, it should be noted that the two decomposition processes of nano FOX-7 were focused in a narrow temperature scope (267.4-280.5℃) compared with the sub-micro FOX-7 (227.7-288.0℃), and raw FOX-7 (227.7-291.1 ℃), which meant that they possessed higher energy release efficiency. Fig. 9 gives the TG curve of the raw and prepared FOX-7. The TG curve of the raw and sub-micro FOX-7 showed three obvious decomposition steps, while nano FOX-7 showed only two vertical steps, identical to the DSC results. TG curve together with the DSC curve shows that nano FOX-7 has a higher decomposition rate than raw and sub-micro FOX-7.

Table 1 Thermal analysis and thermal stability properties of the raw and prepared FOX-7

Entry	APS (μm)	SD (μm)	T_1 (℃)	T_2 (℃)	ΔH (J/g)
Raw	15 μm	4-20	222.7	291.1	937.0
Sub-micro	340nm	0.20-0.45	222,7	288.0	979.0
Nano	78 nm	0.03-0.20	267.4	280.5	1004.0

SD: size distribution, APS: average particle sizes, T_1: The first exothermal peak, T_2: the second exothermal peak.

The total of the exothermal peak of nano FOX-7 (1004J/g) is higher than sub-micro FOX-7 materials (979.0J/g) which is similar with the former works of others,[3,31,55] This still indicates that high energy release of the nano FOX-7 prior to the raw or sub-micro materials. Table 1 provides a comparison of the raw FOX-7 and prepared FOX-7.

4. Conclusions

In conclusion, nano-sized FOX-7 explosive materials were successfully prepared using ultrasonic spray-assisted electrostatic adsorption (USEA) method. The mean particle size of nano FOX-7 is 78 nm and with a narrow particle size distribution in a range of 30-200 nm. The nano sized crystals can be produced continuously and safely via USEA method as a very effective alternative for industrial production. And this method may be used for other energetic materials such as RDX, CL-20 and so on. Different characterization methods show that nano-sized FOX-7 particles prepared by USEA method are faster energy release efficiency and more release energy than the raw FOX-7 and sub-micro FOX-7, because of its less lattice defects and smaller internal stress.

Acknowledgements

This work was supported by the National Natural Science Foundation of China (Project 11002128, 11272292, 11172276, 11202193) and Analytical and Testing center of Southwest University of science and technology.

References

1 A. J. Bellamy, in *High Energy Density Materials*, Springer, 2007, pp. 1-33.
2 A. J. Bellamy, N. V. Latypov and P. Goede, *Journal of Chemical Research*, 2002, **2002**, 257-257.
3 N. V. Latypov, J. Bergman, A. Langlet, U. Wellmar and U. Bemm, *Tetrahedron*, 1998, **54**, 11525-11536.
4 R. J. Hudson, P. Zioupos and P. P. Gill, *Propellants, Explosives, Pyrotechnics*, 2012, **37**, 191-197.
5 J. L. Gottfried, F. C. De Lucia Jr and S. M. Piraino, *DTIC Document*, 2012.
6 R. M. Doherty and D. S. Watt, *Propellants, Explosives, Pyrotechnics*, 2008, **33**, 4-13.
7 C. Zhang, Q. Peng, L. Wang and X. Wang, *Propellants, Explosives, Pyrotechnics*, 2010, **35**, 561-566.
8 F. Nie, J. Zhang, Q. Guo, Z. Qiao and G. Zeng, *Journal of Physics and Chemistry of Solids*, 2010, **71**, 109-113.
9 D. E. Taylor, F. Rob, B. M. Rice, R. Podeszwa and K. Szalewicz, *Physical chemistry chemical physics : PCCP*, 2011, **13**, 16629-16636.
10 Q. FU, Y. SHU and Y. HUANG, *Journal of Solid Rocket Technology*, 2010, **33**, 77-80.
11 H. Ding, Z. Ye, C. Lu, *Chinese Journal of Energetic Materials*, 2012, 20，001-004.
12 R. Andrievski and A. Glezer, *Scripta materialia*, 2001, **44**, 1621-1624.
13 C. Sanchez, G. J. D. A. A. Soler-Illia, F. Ribot and D. Grosso, *Comptes Rendus Chimie*, 2003, **6**, 1131-1151.
14 G. Yang, H. Hu, Y. Zhou, Y. Hu, H. Huang, F. Nie and W. Shi, *Scientific Reports*, 2012, **2**. 1-7
15 V. Stepanov, L. N. Krasnoperov, I. B. Elkina and X. Zhang, *Propellants, Explosives, Pyrotechnics*, 2005, **30**, 178-183.
16 J. T. Essel, A. C. Cortopassi, K. K. Kuo, C. G. Leh and J. H. Adair, *Propellants, Explosives, Pyrotechnics*, 2012, **37**, 699-706.
17 D. Spitzer, C. Baras, M. R. Schäfer, F. Ciszek and B. Siegert, *Propellants, Explosives, Pyrotechnics*, 2009, **36**, 65-74.
18 Z. Yongxu, L. Dabin and L. Chunxu, *Propellants, Explosives, Pyrotechnics*, 2005, **30**, 438-441.
19 Y. Bayat, M. Eghdamtalab and V. Zeynali, *Journal of Energetic Materials*, 2010, **28**, 273-284.
20 H. Qiu, V. Stepanov, T. Chou, A. Surapaneni, A. R. Di Stasio and W. Y. Lee, *Powder Technology*, 2012, **226**, 235-238.
21 G. Yang, F. Nie, H. Huang, L. Zhao and W. Pang, *Propellants, Explosives, Pyrotechnics*, 2006, **31**, 390-394.
22 H. Zhang, J. Sun, B. Kang, Y. Shu, X. Shu, Y. Liu and X. Liu, *Propellants, Explosives, Pyrotechnics*, 2012, **37**, 172-178.
23 V. M. Boddu, D. S. Viswanath, T. K. Ghosh and R. Damavarapu, *J Hazard Mater*, 2010, **181**, 1-8.

24 Y. Bayat and V. Zeynali, *Journal of Energetic Materials*, 2011, **29**, 281-291.
25 J. Li and T. B. Brill, *Propellants, Explosives, Pyrotechnics*, 2006, **31**, 61-69.
26 W. Dun-ju, Z. Jing-lin, W. Jin-ying and W. Bao-guo, *Initiators & Pyrotechnics*, 2007, **1**, 10-14.
27 C. Rossi, K. Zhang, D. Estève, P. Alphonse, P. Tailhades and C. Vahlas, *Microelectromechanical Systems, Journal of microelectromechanical systems* 2007, **16**, 919-931.
28 H. Pezous, C. Rossi, M. Sanchez, F. Mathieu, X. Dollat, S. Charlot, L. Salvagnac and V. Conédéra, *Sensors and Actuators A: Physical*, 2010, **159**, 157-167.
29 B. Wilson, M. Fuchs, D. Gelak, S. Ⅲ and P.Cook, in *53rd Annual NDIA Fuze Conference,Lake Buena Vista*, 2009.
30 C. Rossi, D. Briand, M. Dumonteuil, T. Camps, P. Q. Pham and N. F. d. Rooij, *Sensors and Actuators A: Physical*, 2006, **126**, 241-252.
31 T. Morris, C. Malardier-Jugroot and M. Jugroot, *Journal of Electrostatics*, 2013. **73**, 931-938
32 B. Huang, Z. Qiao, F. Nie, M. Cao, J. Su, H. Huang and C. Hu, *J Hazard Mater*, 2010, **184**, 561-566.
33 T. T. Vo, D. A. Parrish and J. M. Shreeve, *Inorganic chemistry*, 2012, **51**, 1963-1968.
34 A. K. Mandal, U. Thanigaivelan, R. K. Pandey, S. Asthana, R. B. Khomane and B. D. Kulkarni, *Organic Process Research &Development*, 2012, **16**, 1711-1716.
35 H. Cai, L. Tian, B. Huang, G. Yang, D. Guan and H. Huang, *Microporous and Mesoporous Materials*, 2013, **170**, 20-25.
36 C. Koch, *Nanostructured Materials*, 1997, **9**, 13-22.
37 B. Murty and S. Ranganathan, *International materials reviews*, 1998, 43, 101-141.
38 V. M. Rotello, *Nanoparticles*, Springer, 2004.
39 N. Salah, S. S. Habib, Z. H. Khan, A. Memic, A. Azam, E. Alarfaj, N. Zahed and S. Al-Hamedi, *Int J Nanomedicine*, 2011, **6**, 863-869.
40 Q. Zhou, L. Shi, S. Chattoraj and C. C. Sun, *Journal of pharmaceutical sciences*, 2012, **101**, 4258-4266.
41 M. Schoenitz, T. S. Ward and E. L. Dreizin, *Proceedings of the Combustion Institute*, 2005, **30**, 2071-2078.
42 B. Gao, J. Wang, D. Wang, Z. Zhu, Z. Qiao, G. Yang and F. Nie, *International Journal of Nanomedicine*, 2013, **8**, 3927-3936.
43 T. Tillotson, L. Hrubesh, R. Simpson, R. Lee, R. Swansiger and L. Simpson, *Journal of non-crystalline solids*, 1998, **225**, 358-363.
44 A. Shokrolahi, A. Zali, A. Mousaviazar, M. H. Keshavarz and H. Hajhashemi, *Journal of Energetic Materials*, 2011, *29*, 115-126.
45 H. Wang, G. Jian, S. Yan, J. B. DeLisio, C. Huang and M. R. Zachariah, *ACS applied materials & interfaces*, 2013, **5**, 6797-6801.
46 L. Peltonen, H. Valo, R. Kolakovic, T. Laaksonen and J. Hirvonen, *Expert Opinion on Drug Delivery*, 2010, **7**, 705-719.
47 R. J. Lang, *The journal of the acoustical society of America*, 1962, **34**, 6-8.
48 R. Rajan and A. Pandit, *Ultrasonics*, 2001, **39**, 235-255.
49 T. K. McCubbin Jr, *The Journal of the Acoustical Society of America*, 1953, **25**, 1013-1014.
50 E. Rajagopal, *Proceedings Mathematical Sciences*, 1959, **49**, 333-339.
51 B. Avvaru, M. N. Patil, P. R. Gogate and A. B. Pandit, *Ultrasonics*, 2006, **44**, 146-158.
52 A. Guinier, *San Francisco: WH Freeman. HARDMAN-RHYNE, KA & BERK, NF (1985). J. Appl. Cryst*, 1963, **18**, 473-479.
53 A. V. Kimmel, P. V. Sushko, A. L. Shluger and M. M. Kuklja, *The Journal of chemical physics*, 2007, **126**, 234711.
54 A. Gindulyte, L. Massa, L. Huang and J. Karle, *The Journal of Physical Chemistry A*, 1999, **103**, 11045-11051.
55 E. Prodan, *Journal of thermal analysis*, 1984, **29**, 941-948.
56 N. ZOHARI, M. H. KESHAVARZ and S. A. SEYEDSADJADI, *Central European Journal of Energetic Materials*, 2013, **10**, 135-147.
57 A. Burnham, D. Jones, R. Wang, R. Weese and Q. Kwok, *Thermal properties of FOX-7*, United States. Department of Energy, 2005.

A table of contents entry

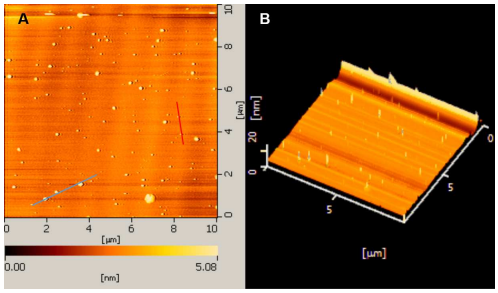

Graphic:

Text: Two kinds of nano FOX-7 particle sizes: elementary particles of about 30-90 nm and 100-200 nm prepared by USEA method.